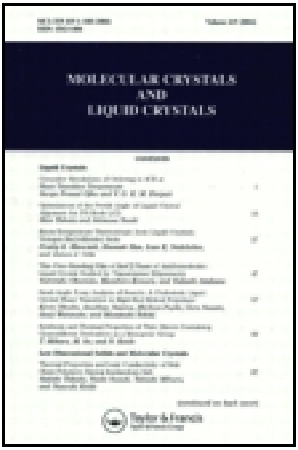

Molecular Crystals and Liquid Crystals
Publication details, including instructions for authors and subscription information:
http://www.tandfonline.com/loi/gmcl20

Europium Complex Incorporated Mesoporous Silica for a Potential pH Sensor

Booyoun An [a] , Sung Soo Park [a] , Yuin Jung [a] , Il Kim [a] & Chang-Sik Ha [a]
[a] Department of Polymer Science and Engineering, Pusan National University, Busan, Korea

To cite this article: Booyoun An , Sung Soo Park , Yuin Jung , Il Kim & Chang-Sik Ha (2008): Europium Complex Incorporated Mesoporous Silica for a Potential pH Sensor, Molecular Crystals and Liquid Crystals, 492:1, 210/[574]-220/[584]

To link to this article: http://dx.doi.org/10.1080/15421400802330697

Mol. Cryst. Liq. Cryst., Vol. 492, pp. 210/[574]–220/[584], 2008
Copyright © Taylor & Francis Group, LLC
ISSN: 1542-1406 print/1563-5287 online
DOI: 10.1080/15421400802330697

Europium Complex Incorporated Mesoporous Silica for a Potential pH Sensor

Booyoun An, Sung Soo Park, Yuin Jung, Il Kim, and Chang-Sik Ha
Department of Polymer Science and Engineering, Pusan National University, Busan, Korea

Highly ordered mesoporous silica, SBA-15 was synthesized using triblock copolymer (P123) as template and tetraethyl orthosilicate (TEOS) as silica source. Through the post-synthesis treatment, pore surface of the mesoporous silica was modified with aminosilane and then Eu^{3+} *ions were incorporated in the modified mesoporous silica for the formation of Eu complex. Mesoporous silica with the hexagonal mesostructure was characterized by small angle X-ray scattering (SAXS) and transmission electron microscopy (TEM). The successful modification of the mesoporous silica was verified by FT-IR spectra and nitrogen adsorption/desorption isotherms. Eu incorporated mesoporous silicas showed different photoluminescent intensities depending on the pH of acidic and basic aqueous solutions.*

Keywords: aminosilane; Eu complex; hexagonal mesostructure; highly ordered mesoporous silica; pH sensor; post-synthesis

INTRODUCTION

Mesoporous silica, named “M41S” and “SBA series”, was synthesized using a surfactant or a triblock copolymer, respectively, as a template to organize the structure of a polymerizing silica precursor [1]. SBA-15 has larger pores (45–300 Å), thicker walls (30–70 Å), and higher thermal stability than does MCM-41 [1(b)]. The structural features of the mesoporous materials – high surface areas ($>1000\,m^2\,g^{-1}$), ordered nanopore structures, narrow pore size distributions and

---

This work was supported by Korea Science and Engineering Foundation (KOSEF) through the National Research Laboratory Program funded by the Ministry of Science and Technology (MOST; No. M10300000369-06J0000-36910), the SRC/ERC program of MOST/KOSEF (Grant #R11–2000–070–080020), and the Brain Korea 21 Project.

Address correspondence to Chang-Sik Ha, Department of Polymer Science and Engineering, Pusan National University, Busan 609-735, Korea. E-mail: csha@pusan.ac.kr

hydroxyl-covered surfaces – make them excellent candidates for the development of new functional materials. These mesoporous molecular sieve materials have found a new range of applications in the areas of catalysis, adsorption, separation, and sensor [2–4]. High sensitivity and ease of operation are two main features for the design and fabrication of a sensor. Fluorescence techniques can be easily fulfill these requirements and fluorescence-based sensors are therefore particularly well suited to monitoring the presence of interesting analytes [5]. Hence, the immobilization of the fluoroionophore for sensing application is of major importance to fabricate an optical sensor device. However the poorly ordered microporosity of such materials is sometimes a limiting factor to the homogeneous and fast diffusion of analytes inside the sensing matrix, usually leading to rather long response time [6]. On the other hand, with recent advances in mesostructured materials and nanotechnologies, new methods are emerging to develop highly sensitive fluorescent chemosensing materials [7]. Wirnsberger *et al.* [8] and Li *et al.* [9] reported pH sensing phenomena using organic dye-functionalized mesoporous silica in mesopores. The emission spectrum of europium(III) complexes is particularly sensitive to the local coordination environment provided by the ligand. Both the local symmetry around the metal and the charge and polarizability of the donor atoms determine the relative intensity of the emission bands from the $^5D_0$ excited state. Gunnlaugsson *et al.* [10] reported a pH sensing phenomenon using Eu(III) complex molecules in a highly acidic environment.

In this work, we present a pH sensing phenomenon in base environment using europium complex incorporated mesoporous silica, SBA-15.

EXPERIMENTAL

Tetraethyl orthosilicate (TEOS), Poly (ethylene oxide)-*block*-poly(propylene oxide)-*block*-poy(ethylene oxide) ($PEO_{20}PPO_{70}PEO_{20}$: P123, Mn = 5800), N-[3-(trimethoxysilyl)propyl]ethylenediamine ($(CH_3O)_3Si(CH_2)_3NHCH_2CH_2NH_2$:APTMS), Europium(III) chloride hexahydrate ($EuCl_3 \cdot 6H_2O$), Chloroform ($CHCl_3$) were purchased from Aldrich and used without further purification. Hydrochloric acid (HCl) was purchased from Junsei and used as received.

Synthesis of Highly Ordered Mesoporous Silica, SBA-15 [1(b)]

In a typical synthesis, 16 g of triblock copolymer (P123) was dissolved in 500 g of water and 80 g of 35 wt% HCl with stirring at 35°C until homogeneous solution was observed. Then 34.4 g of TEOS was added into this homogeneous solution and the mixture was stirred for 15 min. And the mixture was aged for 24 h at the same temperature under static condition. Subsequently, the mixture was heated at 100°C for 24 h under static condition. The solid products were collected by filtration, washed thoroughly with water several times, and dried at 80°C. The as-synthesized sample was calcined at 550°C for 4 h in air.

Preparation of Modified Mesoporous Silica, SBA-15 [11]

N-[3-(trimethoxysilyl)propyl]ethylenediamine (APTMS) was used to modify the inner wall surfaces of mesoporous silica. To remove water which is bonded with surface silanol groups, the SBA-15 samples were degassed at 300°C for 5 h under vacuum condition. 0.1 g of degassed samples were dispersed in 0.1 M of APTMS chloroform solution and stirred at room temperature for 12 h. The products were filtered, washed with chloroform several times and dried at 80°C. This sample was named "APTMS/SBA-15".

Incorporation of Eu^{3+} ions into the Modified Mesoporous Silica, SBA-15

0.1 g of APTMS/SBA-15 was dispersed in 0.04 M of Europium(III) chloride aqueous solution and stirred at room temperature for 2 h. The final products were collected by filtration, washed thoroughly with water several times and dried at 80°C. This sample was named "Eu/APTMS/SBA-15".

Characterization

Small angle X-ray scattering (SAXS) was performed at Pohang Accelerator Laboratory (PLA), POSTECH, Korea with Co Kα ($\lambda = 1.608$ Å) radiation. TEM images were recorded on a JEOL 2010 electron microscope operating at 200 kV. Nitrogen adsorption/desorption isotherms were measured at 77K using a Nova 4000e instrument. Prior to measurement samples were dehydrated at 150°C for 5 h. The BET (Brunauer-Emmett-Teller) method was used to calculate the specific surface area. The pore size distribution was calculated from the analysis of the desorption branch of the isotherm by BJH (Barrett-Joyner-Halenda) method. FT-IR spectra of samples in KBr pellets were obtained using a Shimadzu IR Prestige-21 spm. The photoluminescence (PL) spectra were measured with HITACHI Instrument F-4500 spectrophotometer equipped with a xenon lamp.

RESULTS AND DISCUSSTION

Figure 1 shows SAXS patterns of (a) calcined SBA-15, (b) APTMS/SBA-15, and (c) Eu/APTMS/SBA-15 samples. All SAXS patterns exhibit five well-resolved peaks (a prominent peak at 0.68, 1.18, 1.36 nm^{-1} and two weak peaks at 2.04, 2.36 nm^{-1}) that can be indexed as the (100), (110), (200), (220), and (300) reflections of *p6mm* hexagonal symmetry with lattice *d*-spacing of 9.2, 5.3, 4.6, 3.1, and 2.7 nm, respectively [1(b)]. The corresponding unit cell parameter, a_0, is 10.6 nm ($a_0 = 2d_{100}/\sqrt{3}$). Comparision of the SAXS patterns clearly shows that the modification of APTMS and incorporation of Eu^{3+} in mesopores does not affect the SBA-15 mesostructure. However, slight decreases of the relative reflection intensities of (100) peaks and other minor peaks were observed after modification of SBA-15 with APTMS. The decrease in the peak intensities are due to filling of the pores of SBA-15 during the incorporating process because such pore filling reduces the scattering contrast between the pores and the walls of a mesoporous material.

Figures 2(a) and 2(b) show TEM images of the calcined SBA-15 have well ordered hexagonal array channel structure. In Figures 2(c) and 2(d), Eu/APTMS/SBA-15 sample also has highly ordered and well defined structures. It reveals that the samples are very stable and

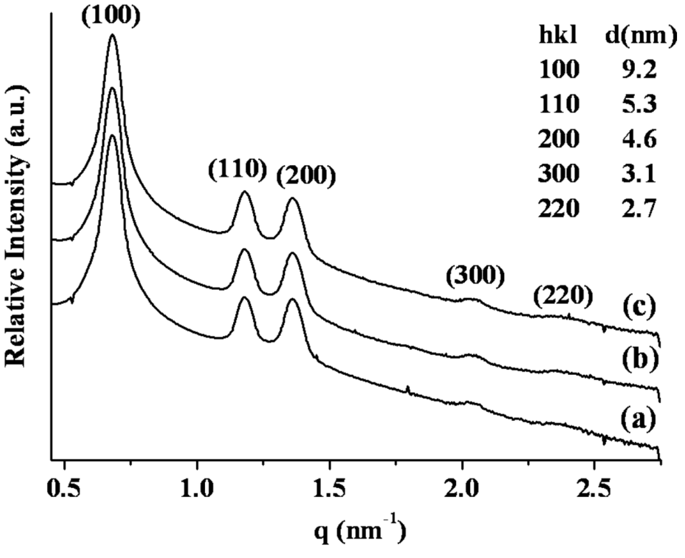

FIGURE 1 SAXS patterns of (a) calcined SBA-15, (b) APTMS/SBA-15, and (c) Eu/APTMS/SBA-15.

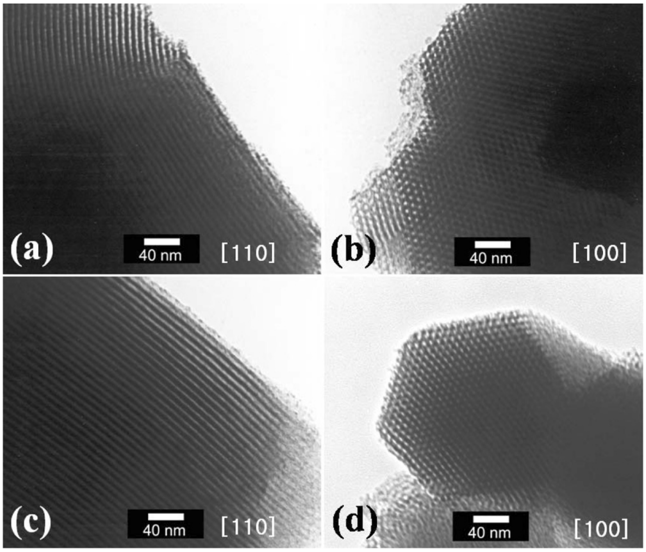

FIGURE 2 TEM images of (a, b) calcined SBA-15 and (c, d) Eu/APTMS/SBA-15.

thus the structures are well preserved after post-synthesis treatment. One more important point is that any clusters of Eu complexes do not exist around mesopores. It indicates that Europium ions well dispersed in the pores and were not on the external surface of pores.

Figure 3 shows the nitrogen adsorption/desorption isotherm curves of the (a) calcined SBA-15 and (b) Eu/APTMS/SBA-15 samples. After incorporation of Eu^{3+} into the modified SBA-15 channel (i.e., for Eu/APTMS/SBA-15), we observed a decrease in the amount of nitrogen adsorbed and a shift in the inflection point of the step to a smaller relative pressure (Figure 3(b)). We attributed the reduced nitrogen adsorption to the smaller specific surface area and the lower relative pressure to the decreased pore size, respectively [12]. After incorporation of Eu^{3+} within the mesoporous channels, the pore diameter decreased from 67 Å to 52 Å (Inset in Figure 3). These results indicate that Eu^{3+} ions were incorporated successfully into the modified SBA-15 channels.

Figure 4 shows IR spectra of (a) calcined SBA-15, (b) APTMS/SBA-15, and (c) Eu/APTMS/SBA-15 [11]. The peaks at $803\,cm^{-1}$ and $1079\,cm^{-1}$ can be attributed to symmetric Si-O and the asymmetric Si-O stretching vibration. The Si-O-Si bending vibration can be observed at $463\,cm^{-1}$, and the bands at $965\,cm^{-1}$ can be assigned to

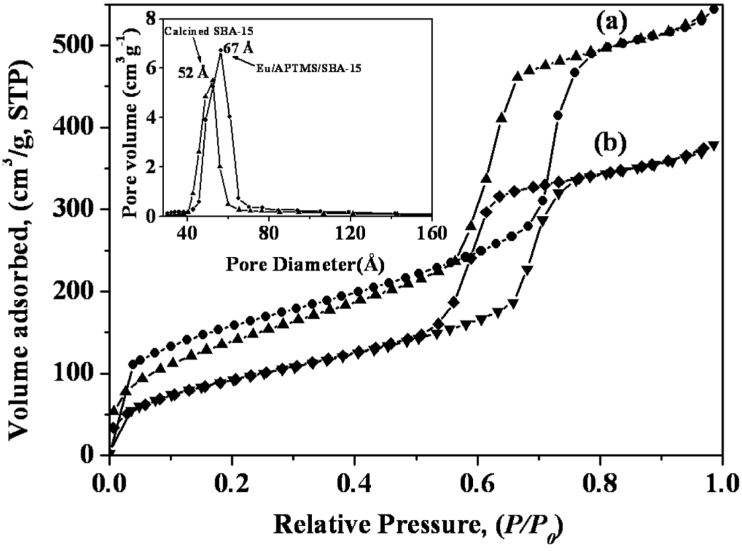

FIGURE 3 Nitrogen adsorption/desorption isotherm curves of the (a) calcined SBA-15 and (b) Eu/APTMS/SBA-15. Inset shows pore size distribution of calcined SBA-15 and Eu/APTMS/SBA-15.

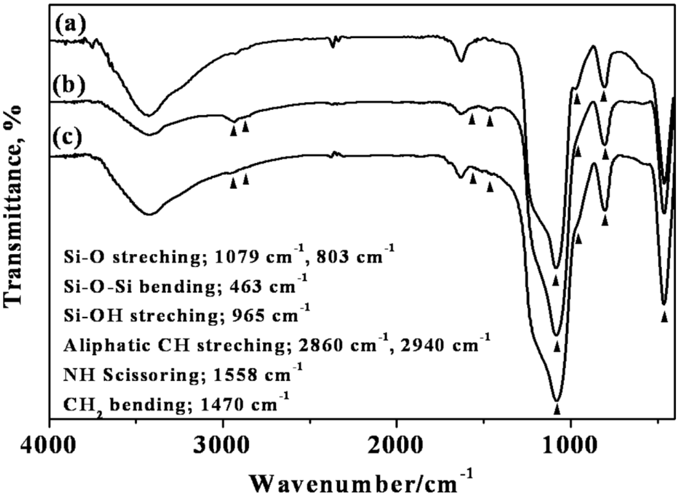

FIGURE 4 IR spectra of (a) calcined SBA-15, (b) APTMS/SBA-15, and (c) Eu/APTMS/SBA-15.

stretching vibrations of Si-OH groups. After pore surface modification by aminosilane (Fig. 4(b)), both 2860 cm^{-1} and 2940 cm^{-1} for aliphatic CH stretching, 1558 cm^{-1} for NH scissoring, 1470 cm^{-1} for CH_2 bending can be assigned. On the other hand, the 965 cm^{-1} peak for Si-OH groups of SBA-15 was decreased remarkably. This is due to the formation of Si-O-Si linkage between aminosilane and Si-OH group. Also, Eu/APTMS/SBA-15 (Fig. 4(c)) displays similar IR spectra to APTMS/SBA-15 (Fig. 4(b)). The results of IR analysis also strongly supports successful post synthesis treatment.

Figure 5 shows photoluminescence (PL) spectra of (a) calcined SBA-15, (b) APTMS/SBA-15, and (c) Eu/APTMS/SBA-15. In Figure 5(c), four emission peaks in the Eu/APTMS/SBA-15 arise from transitions between $^5D_1 \rightarrow ^7F_J$ crystal field components (J = 1, 2, 3, 4). The characteristic emission peaks appearing in the spectrum correspond to the transition $^5D_0 \rightarrow ^7F_1$ (588.9 nm), $^5D_0 \rightarrow ^7F_2$ (611.6 nm), $^5D_0 \rightarrow ^7F_3$ (649.3 nm) and $^5D_0 \rightarrow ^7F_4$ (696.7 nm) and any other peaks were not appeared for the calcined and modified SBA-15 [13].

Figure 6 shows PL spectra of Eu/APTMS/SBA-15 samples with different content of Eu^{3+} ion. The intensity of the $^5D_0 \rightarrow ^7F_2$ transition peak of each sample was plotted as a function of Eu^{3+} ion concentration. This concentration dependency means that Eu^{3+} ions

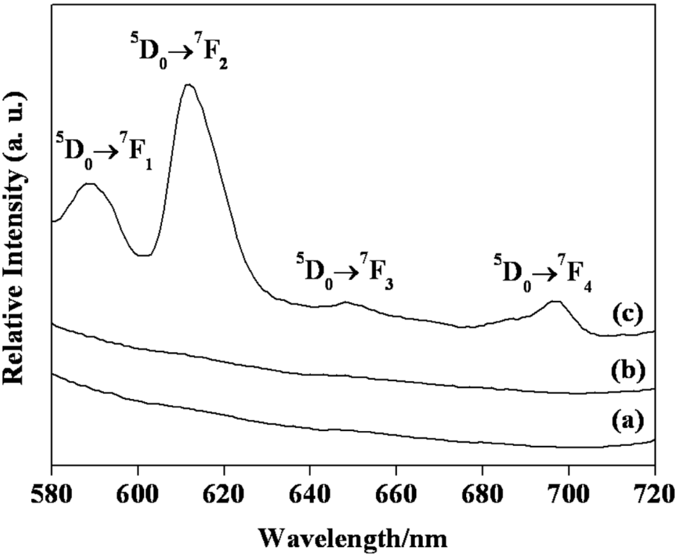

FIGURE 5 Photoluminescence (PL) spectra of (a) calcined SBA-15, (b) APTMS/SBA-15, and (c) Eu/APTMS/SBA-15.

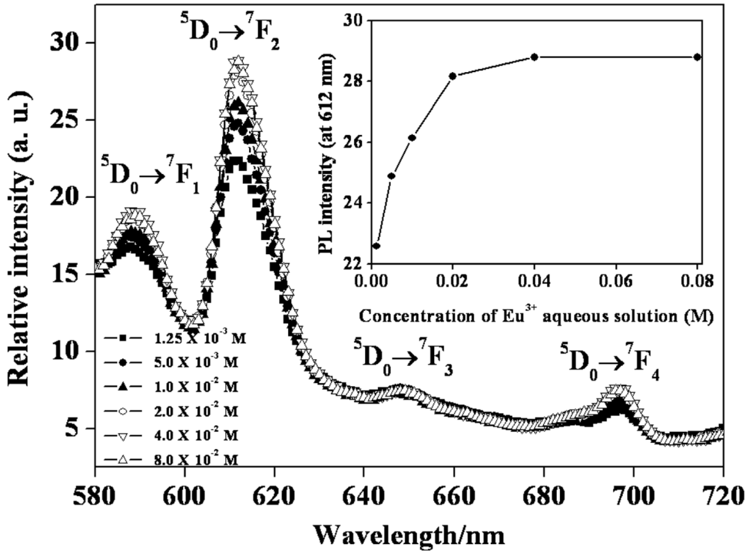

FIGURE 6 Photoluminescence (PL) spectra of Eu/APTMS/SBA-15 with different content of Eu^{3+} ion. Inset shows the PL intensity at 612 nm of Eu/APTMS/SBA-15 prepared with different concentration of Eu^{3+} aqueous solutions.

have been effectively incorporated into modified mesoporous silica pores, which reduces the concentration quenching. Also, the content of Eu^{3+} ions can be controlled by changing the molar concentration of Eu complex aqueous solutions (Inset in Fig. 6). From this result, 4.0×10^{-2} M was used as standard molar concentration for the experiment.

Figure 7 shows PL spectra of Eu/APTMS/SBA-15 in NaOH aqueous solutions with different pH values. Eu/APTMS/SBA-15 shows remarkably different PL behavior depending on different pH of the NaOH aqueous solutions. With the increase from $pH = 6.5$ to 12.5, the peak intensity of the PL spectra decreased. In particular, the peak intensity of $^5D_o \rightarrow {}^7F_2$ transition was changed clearly with the different pH values. This result is due to the deactivation of exited Eu complex in base solution by means of vibrational energy transfer to high energy vibrations [14]. In a sense, Eu^{3+} ions formed Eu-amine complexes (Eu/APTMS/SBA-15) in mesopores of aminosilane-modified SBA-15 (APTMS/SBA-15). And, the Eu complexes may contain several H_2O molecules. Then, H_2O molecules are displaced by binding OH^- ions as quenching oscillators in base solution. Therefore, the emission

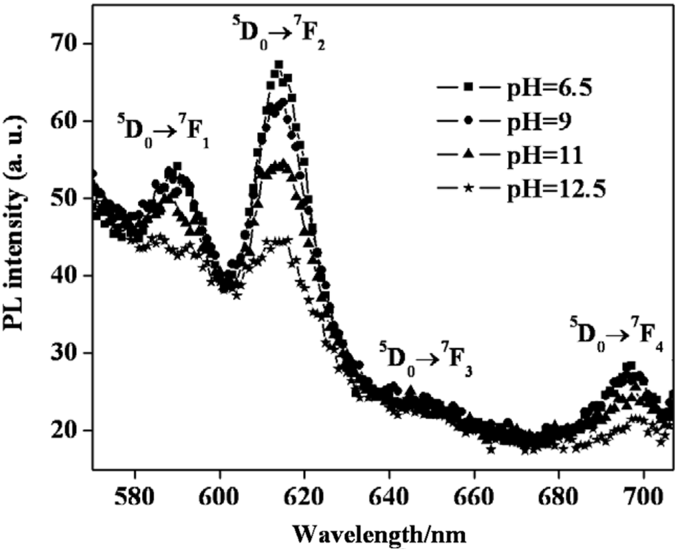

FIGURE 7 Photoluminescence (PL) spectra of Eu/APTMS/SBA-15 in NaOH aqueous solutions with different pH values.

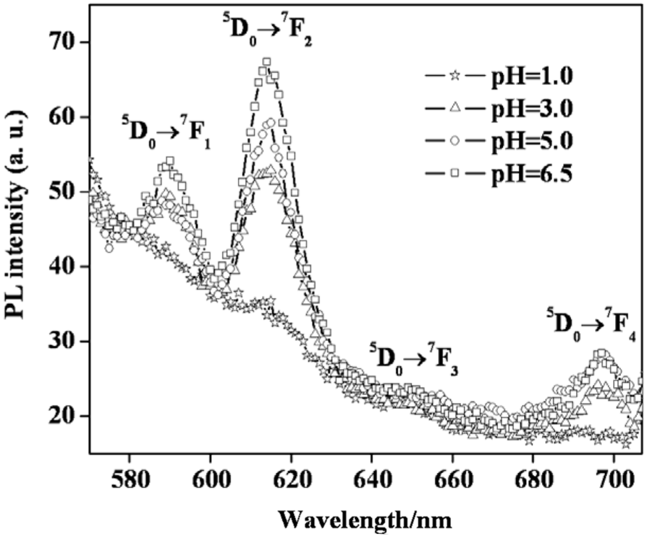

FIGURE 8 Photoluminescence (PL) spectra of Eu/APTMS/SBA-15 in HCl aqueous solutions with different pH values.

peak intensity of Eu/APTMS/SBA-15 is decreased while pH values are increased in NaOH aqueous solutions.

Figure 8 shows PL spectra of Eu/APTMS/SBA-15 in HCl aqueous solutions with different pH values. Interestingly, with the decrease of pH from 6.5 to 1, the peak intensity of the PL spectra was also decreased. In particular, the peak intensity of the $^5D_o \rightarrow {}^7F_2$ transition was changed clearly with the decrease of pH values from $pH = 6.5$ to 1. This result may be due to the partial formation of amine salt between amines in the APTMS functional group and H^+ ions at low pH, for instance, $pH = 1$. Also, the Eu complexes may contain several H_2O molecules as quenching oscillators in acid solution. Therefore, the emission peak intensity of the Eu/APTMS/SBA-15 is decreased while pH values are changed from $pH = 6.5$ to 1 in HCl aqueous solutions. Recently, Pal and Parker reported Eu(III) complex incorporating an *N*-methylsulfonamide moiety can work as a pH probe [15].

In this work, even after the treatment of Eu/APTMS/SBA-15 in $pH = 1 \sim 12.5$, Eu(III) ions were not released from mesopores, which were confirmed by their PL spectra.

CONCLUSIONS

By the post-synthesis method, mesopores of highly ordered mesoporous silica were modified with aminosilane and then Eu^{3+} ions were incorporated in the modified mesoporous silica for the formation of Eu complex. PL spectra of the Eu incorporated mesoporous silica showed pH dependency of PL intensity in the acidic and basic aqueous solutions of different pHs. From this result, Eu incorporated mesoporous silica may be expected to be applied as pH sensor or detector.

REFERENCES

[1] (a) Kresge, C. T., Leonowicz, M. E., Roth, W. J., Vartuli, J. C., & Beck, J. S. (1992). *Nature*, *359*, 710; (b) Zhao, D., Feng, J., Huo, Q., Melosh, N., Fredrickson, G. H., Chmelka, B. F., & Stucky, G. D. (1998). *Science*, *279*, 548.

[2] Sayari, A. (1996). *Chem. Mater.*, *8*, 1840.

[3] Raimondo, M., Perez, G., Sinibaldi, M., de Stefanis, A., & Tomlinson, A. A. G. (1997). *Chem. Commun.*, *15*, 1343.

[4] Grün, M., Kruganoz, A. A., Schacht, S., Schüth, F., & Unger, K. K. (1996). *J. Chromatogr. A*, *740*, 1.

[5] Mason, W. T. (1999). *Fluorescent and Luminescent Probes for Bilogical Activity*, Ch. 2, p. 17. Academic Press: San Diego, USA.

[6] Rottman, C., Ottolenghi, M., Zusman, R., Lev, O., & Crego-Calama, M. (2005). *Chem. Mater.*, *15*, 2657.

[7] (a) Canada, T. & Xue, Z. L. (2002). *Asnal. Chem.*, *74*, 6073; (b) Zimmerman, R., Basabe-Desmonts, L., van der Baan, F., Reinhoudt, D., & Crego-Calama, M. (2005). *J. Mater. Chem.*, *15*, 2772; (c) Palomares, E., Vilar, R., Green, A., & Durrant, J. R. (2004). *Adv. Funct. Mater.*, *14*, 111; Beer, P., Cormode, D., & Davis, J. (2004). *Chem. Commun.*, *4*, 414.

[8] Wirnsberger, G., Scott, B. J., & Stucky, G. D. (2001). *Chem. Commun.*, 119.

[9] Li, L. L., Sun, H., Fang, C.-J., Xu, J., Jin, J.-Y., & Yan, C.-H. (2007). *J. Mater. Chem.*, *17*, 4492.

[10] Gunnlaugsson, T. (2001). *Tetra. Lett.*, *42*, 8901.

[11] Park, D. H., Park, S. S., & Choe, S. J. (1999). *Bull. Korean Chem. Soc.*, *20*, 291.

[12] Zhao, D., Huo, Q., Feng, J., Chmelka, B. F., & Stucky, G. D. (1998). *J. Am. Chem. Soc.*, *120*, 6024.

[13] Li, H., Lin, J., Zhang, H., Fu, L., Meng, Q., & Wang, S. (2002). *Chem. Mater.*, *14*, 3651.

[14] Parker, D. (2000). *Cood. Chem. Rev.*, *205*, 109.

[15] Pal, R. & Parker, D. (2007). *Chem. Commun.*, *5*, 474–476.